

Biomanufacture of nano-Pd(0) by *Escherichia coli* and electrochemical activity of bio-Pd(0) made at the expense of H₂ and formate as electron donors

J. Courtney · K. Deplanche · N. V. Rees ·
L. E. Macaskie

Received: 29 May 2016 / Accepted: 19 July 2016
© The Author(s) 2016. This article is published with open access at Springerlink.com

Abstract

Objective Palladised cells of *Desulfovibrio desulfuricans* and *Shewanella oneidensis* have been reported as fuel cell electrocatalysts but growth at scale may be unattractive/costly; we have evaluated the potential of using *E. coli*, using H₂/formate for Pd-nanoparticle manufacture.

Results Using ‘bio-Pd’ made under H₂ (20 wt%) cyclic voltammograms suggested electrochemical activity of bio-NPs in a native state, attributed to proton adsorption/desorption. Bio-Pd prepared using formate as the electron donor gave smaller, well separated NPs; this material showed no electrochemical properties, and hence little potential for fuel cell use using a simple preparation technique. Bio-Pd on

S. oneidensis gave similar results to those obtained using *E. coli*.

Conclusion Bio-Pd is sufficiently conductive to make an *E. coli*-derived electrochemically active material on intact, unprocessed bacterial cells if prepared at the expense of H₂, showing potential for fuel cell applications using a simple one-step preparation method.

Keywords Bio-Pd · *E. coli* · Electrochemical activity · Fuel cell · Hydrogen production · Palladium

Introduction

A proton electrolyte membrane fuel cell (PEM-FC) comprises anode and cathode catalysts separated by a proton exchange membrane. Catalytic splitting of H₂ anodically provides electrons, which recombine with protons and atmospheric O₂ at the cathode, forming water. Alternatively, microbial fuel cells can generate electricity from waste (e.g. Wu et al. 2014; Sanchez et al. 2015) but the low power density limits their use (Jang et al. 2013). Bacteria can make H₂ from waste to supply the anodic reaction (Macaskie et al. 2005; Redwood et al. 2012); residual bacteria can then make metallised FC-catalyst biomaterial with precious metals biorecovered from waste (Orozco et al. 2010).

Yeast (Dimitriadi et al. 2007) or bacterial (Yong et al. 2007) cells support palladium nanoparticle

N. V. Rees · L. E. Macaskie (✉)
School of Biosciences, University of Birmingham,
Edgbaston, Birmingham B15 2TT, UK
e-mail: L.E.Macaskie@bham.ac.uk

N. V. Rees
e-mail: N.Rees@bham.ac.uk

Present Address:
J. Courtney
School of Chemistry, University of East Anglia, Norwich
Research Park, Norwich, Norfolk NR4 7TJ, UK
e-mail: j.courtney@uea.ac.uk

Present Address:
K. Deplanche
Finovatis, 68 Cours Lafayette, 69003 Lyon, France
e-mail: K.deplancheb@gmail.com

(Pd-NP) PEM-FC electrodes; the biomaterial required sintering (carbonisation) to improve conductivity (Yong et al. 2007). The highest power output, comparable to commercial FC catalyst, used sintered, platinised cells of *Desulfovibrio desulfuricans*, (Yong et al. 2007) but palladised sintered cells of *D. desulfuricans* and also *E. coli* (bio-Pd_{D. desulfuricans} and bio-Pd_{E. coli}) were also active (Yong et al. 2010).

Later work showed electrochemical activity of palladised native cells of *D. desulfuricans*, increased by adding formate (electron donor) to live, but not heat-killed cells while lactate supported activity using bio-Pd on live cells only; cytochromes and periplasmic hydrogenases were implicated (Wu et al. 2011). Similarly, Ogi et al. (2010) used Pd-NPs on cells of *Shewanella oneidensis* in a PEM-FC to give a power output of 90 % of that of a commercial catalyst at a Pd loading of 20 % of the biomass dry weight. Studies have focused on the anodic reaction whereas the rate-limiting cathodic O₂ reduction reaction (ORR) is relatively unexplored. Non-metallised, active cells were used cathodically, with limited success (Jang et al. 2013). Williams (2016) achieved the ORR by using bio-Pt_{E. coli}, comparably to a commercial FC catalyst, following chemical stripping of biochemical components to unmask an electrochemically-responsive Pt surface (Attard et al. 2012).

Substitution of Pd into the electrodes would offer major cost benefits. A PEM-FC with a ‘bio-Pd’ anode (Yong et al. 2007, 2010) gave consistent power output over several weeks although Pd is generally held to have a short catalyst life; durability targets are 5000 h of operation for automotive application and 40,000 h for stationary FCs over 10 years (Rice et al. 2015).

D. desulfuricans is not readily scalable; it is difficult to grow to high cell densities, while the removal of H₂S (a powerful catalyst poison) is required; this restriction could also apply to *S. oneidensis* which produces H₂S from various sulfur compounds (Wu et al. 2015). Practically, one could use an organism grown aerobically to high cell densities (e.g. waste bacteria from other applications). Hydrogenases, [which make bio-Pd (Deplanche et al. 2010)], are then upregulated during anaerobic resuspension for catalyst manufacture (Zhu et al. 2016).

Yong et al. (2007, 2010) and Ogi et al. (2011) agreed that maximum FC-activity requires a high loading of Pd(0) (20 wt%). Native palladised cells of *D. desulfuricans* were active in electron transport (Wu

et al. 2011) but the Pd(0)-loading was not stated; it may be possible to use native bio-Pd_{E. coli} electrocatalytically, given suitable conductivity. This study compared bio-Pd_{E. coli} in two ways using voltammetry to assess electrochemical activity. Successful proof would open the harnessing of ‘2nd life’ *E. coli* biomass into new catalysts, using these bacteria to make FC catalysts from metallic wastes (above) as well as potentially harnessing the tools of synthetic biology towards ‘designer’ catalysts, since *E. coli* is the ubiquitous ‘workhorse’ organism for molecular engineering.

Materials and methods

Cell culture

E. coli MC4100 was as described previously (Deplanche et al. 2010). Cultures were grown anaerobically in sealed bottles in lysogeny broth (LB) (10 g tryptone/l, 5 g yeast extract/l, 10 g NaCl/l). Cultures were harvested by centrifugation in the mid-logarithmic phase of growth (OD₆₀₀ of 0.5–0.7), washed three times in 100 ml 20 mM MOPS/NaOH buffer (degassed, pH 7.2) and resuspended in a small volume of the same buffer (4 °C) until use, usually the next day. Cell concentration (mg/ml) was determined by reference to a pre-determined OD₆₀₀ to dry weight conversion. Some tests used *Shewanella oneidensis* strain MR1 grown and prepared in the same way.

Palladium mineralisation

To make bio-Pd, 25 ml concentrated resting cell suspension was transferred under O₂-free N₂ into 200 ml serum bottles and 40 ml degassed 10 mM Pd(II) [sodium tetrachloropalladate (Na₂PdCl₄ in 0.01 M nitric acid, aq.)], or palladium chloride (PdCl₂ in 0.01 M HNO₃) was added to give a final loading of 20 % (w/w) Pd on biomass. Pd/cells were left to stand (30 min, 30 °C) with occasional shaking to promote biosorption of Pd(II) complexes before either H₂ was sparged through the suspension (200 ml/min, 20 min) or 5 ml 50 mM sodium formate (degassed) was added to reduce cell surface-bound Pd(II) to Pd(0). To confirm the metal content of the metal/cell catalysts, the residual free Pd(II) ion content in solution was monitored at all stages of the

preparation spectrophotometrically using the tin chloride method (Deplanche et al. 2010).

Electron microscopy

For scanning transmission electron microscopy (STEM), the Pd cell samples were immersed in 2.5 % glutaraldehyde (1 day). Secondary fixation used 1 % OsO₄ (1 h; omitted where analysis was to be done using energy dispersive X-ray microanalysis (EDS)). Samples were dehydrated using 50, 70, 90 and 100 % ethanol (2 × 15 min for each). Two further dehydration steps (15 min) were made in propylene oxide and samples were embedded in a 1:1 mixture of propylene oxide/resin (45 min; gentle shaking) then pure resin (1 h, then *in vacuo*; 30 min) and cured (60 °C; >16 h; atmospheric pressure). For STEM, samples were cut into thin sections (diamond knife; 50–150 nm) and collected on electron microscope girds (Formvar film/carbon coated). Standard stains of uranyl acetate and lead citrate were added and the samples were examined using a Jeol JSM-7000f FE-SEM with an Oxford Inca EDS detector.

Electrochemical analysis of bio-Pd(0) prepared under H₂ or with formate

Working electrodes were made using the drop-cast technique. A 3 mm (EDI101, Radiometer Analytical, Salford, UK) and 5 mm diameter (afe2m050gc, Pine Research Instrumentation, Durham) glassy carbon rotating disc electrode (RDE) tip was taken and 20 µl (5 mm) or 10 µl (3 mm) of bio-Pd suspension was deposited onto a polished tip. The tip was covered with a beaker and left to dry (12 h). A three electrode half-cell set-up was used with a surrounding water jacket (25 °C). The reference electrode (RE) was a normal H₂ electrode (NHE), the counter electrode (CE) was platinum gauze and the working electrode (WE) was as above. The WE was connected to an Autolab (PGStat302N, Metrohm-Autolab, Utrecht, The Netherlands) potentiostat/galvanostat through either a EDI101 RDE (Radiometer Analytical, 3 mm) or a Pine modulated speed rotator (AFMSRCE, Pine Research Instrumentation, 5 mm). The electrolyte was 0.1 M perchloric acid (Sigma-Aldrich, *TraceSELECT* Ultra), with a N₂ purge (20 min). Prior to electrochemical analysis the electrode was ‘cleaned’ by cycling the applied potential between 0

and 1.1 V (vs. NHE) (50 cycles at 0.1 V/s). The WE was then placed in the half-cell described above and cyclic voltammetry (CV) data was recorded by applying potential scans between 0 and 1.1 V (vs. NHE) at various scan rates (0.1, 0.5, 0.05, 0.025 V/s).

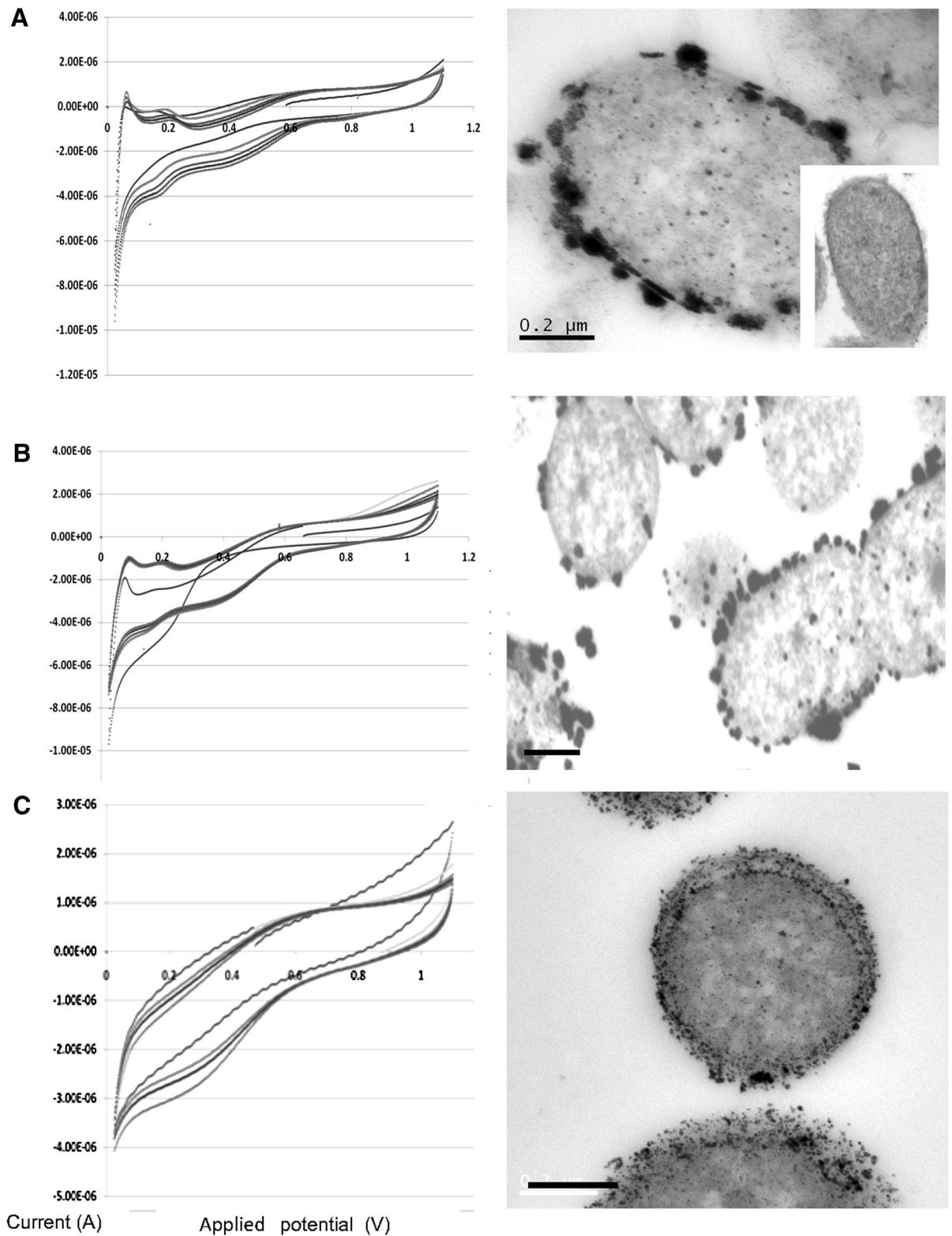
Results and discussion

Uptake of Pd(II) from solution

Initial tests compared the rate of reduction of Pd(II) from Na₂PdCl₄ solutions using H₂ or formate as electron donors following the initial biosorption of Pd(II). Under H₂ complete removal of Pd(II) was invariably observed within 5–10 min whereas the removal of Pd(II) via formate required ~1 h. By substituting PdCl₂ for Na₂PdCl₄ the rate of Pd(II) reduction was doubled, possibly attributable to a greater predominance of Pd²⁺ ions at the lower concentration of chloride, i.e. with less tendency to form neutral (PdCl₂) or anionic (PdCl₃[−]) species in solution. Since Pd(II) can behave in a similar way to Ni(II), it is possible that cellular uptake and trafficking mechanisms for Ni(II) may have facilitated uptake of Pd(II) into the cells although the route of Pd(II) uptake following initial biosorption, and the effect of Pd(II) ions, remain to be confirmed, along with any increased toxicity effects of the 10 mM Pd(II) as used in this study [previous work has generally used 2 mM Pd(II)].

Biodeposition of Pd(0) on bacterial cells

Material made from PdCl₂ under H₂ showed large Pd-NPs (Fig. 1a; confirmed as Pd by EDS; not shown) not visible on Pd-unchallenged cells (inset). Some deposits showed co-localisation in the outer and inner membranes. A similar pattern of Pd-deposition was obtained using Na₂PdCl₄ (Fig. 1b). The Pd-NPs made under H₂ were generally smaller when made using Na₂PdCl₄ (Fig. 1b) than with PdCl₂ (Fig. 1a). Those made using formate were very small (Fig. 1c) and were indistinguishable with respect to the palladium salt used (Fig. 2b, c) but were more numerous than those made under H₂ (Figs. 1, 2a). A closer examination of the deposited NPs (Fig. 2) reveals morphological differences. NPs made under H₂ appear large but comprised, in some cases, agglomerations of small



◀ **Fig. 1** Formation of Pd-nanoparticles (20 wt%) on *E. coli* MC4100 using H₂ and formate as electron donors (*right panels*) and cyclic voltammograms of the palladised cell preparations (*left panels*; multiple lines denote repeated scans). **a** H₂ as electron donor for synthesis of Pd(0) from PdCl₂ as the Pd(II) salt. *Inset* cells unchallenged with Pd(II). **b** H₂ as electron donor for synthesis of Pd(0) from Na₂PdCl₄ as the Pd(II) salt. **c** Formate as electron donor for synthesis of Pd(0) from Na₂PdCl₄ as the Pd(II) salt. *Bars* 200 nm

NPs, visible as separate entities (Fig. 2a). In contrast NPs made via formate were small and well separated (Fig. 2b, c).

We suggest that the use of formate is rate-limiting due to the need to split it into H₂ and CO₂ in order to reduce Pd(II) at the expense of generated H₂. This can occur either autocatalytically by ‘seeds’ of Pd(0) that split formate catalytically, or enzymatically using formate H₂ lyase (FHL). However, FHL is not a periplasmic enzyme, which is in contradiction to the localisation of most of the NPs seen by electron microscopy (Figs. 1c, 2b, c). FHL activity may be involved in intracellular Pd-NP deposition; some Pd-NP deposits are visible intracellularly as well as in association with the inner membrane (Fig. 1). If the Pd-NP synthesis reaction is limited by the rate of formate cleavage it is likely that some Pd(II) persists at the cell surface long enough for it to localise onto additional potential nucleation sites rather than rapid initial nucleation and consolidation onto fewer sites, nearer to the cell surface, when promoted by H in a fast reaction.

A detailed study of the roles of hydrogenases in the pattern of deposition of Pd(0) by *E. coli* was reported (Deplanche et al. 2010). Unlike *Desulfovibrio*, which

has periplasmic hydrogenases involved in Pd(0) deposition (Mikheenko et al. 2008), those of *E. coli* are cytoplasmic membrane-bound, with the inward-facing hydrogenase 3 component of the FHL complex making cytoplasmic-facing Pd(0). Such an arrangement is visible on the inner membrane of the cells in Fig. 1c, confirmed elsewhere using a mutant which expressed only hydrogenase 3 (Deplanche et al. 2010). In contrast the inner membrane-localisation of Pd(0) when made under H₂ evidenced more discrete, denser depositions (Fig. 1a). Deplanche et al. (2010) showed that there is no single hydrogenase involvement in Pd(0) manufacture by *E. coli*; several hydrogenases are involved, the size of the Pd-nanoparticles relating to the enzyme that produced them. A similar result was reported using *D. fructosovorans* (Mikheenko et al. 2008). Other work, in contrast to this study and using *S. oneidensis*, suggested that, with formate, Pd-NPs were larger (and fewer) than by using H₂ (de Windt et al. 2005) but de Windt et al. (2006) also showed size control of Pd-NPs according to the conditions. Søbjergr et al. (2011) reported that NPs can be size-controlled by adjusting the biomass/Pd ratio while Williams (2016) showed, with bio-Pd_{D. desulfuricans}, that, by using the same biomass (mg)/metal (total atoms) ratio, different NP sizes resulted according to whether a small volume of 10 mM Pd(II) was used (i.e. as in this study), or a fivefold more dilute solution (2 mM, as in other work). This suggests that metal toxicity (i.e. metal concentration) may play a role in determining the number of loci that go on to support NP growth if this is enzymatically-mediated. The involvement of other enzymes than hydrogenases is not precluded; hydrogenase-deficient mutants of *E. coli* made Pd(0)

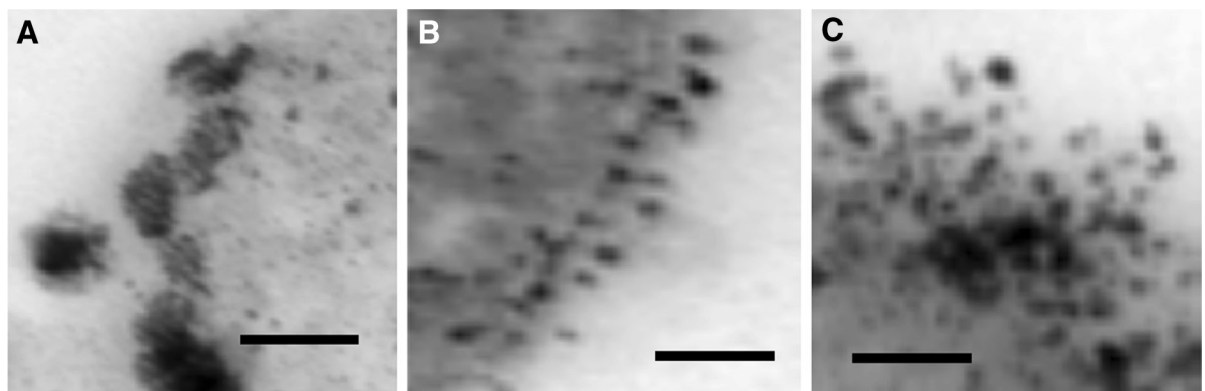


Fig. 2 Detail of Pd-nanoparticles formed on the surface of *E. coli* at 20 wt% loading at the expense of **a** H₂ + PdCl₂; **b** formate + PdCl₂ and **c** formate + Na₂PdCl₄. *Bar* 100 nm

but this was localised as fewer, larger NPs on the cell surface (Deplanche et al. 2010).

Electrochemical analysis of bio-Pd(0) made at the expense of H₂ and formate

CV has been used to probe the crystal surface structure of bio-Pt. (Attard et al. 2012). Using bio-Pd made under H₂ CV gave evidence for electrochemical activity of the bio-NPs in a native (non-sintered) state (Fig. 1a, b), attributed to the adsorption/desorption of protons, and indicating an electrochemically active surface area and so a routine test for fuel cell catalysts. In contrast bio-Pd prepared using formate as the electron donor gave well separated NPs, with the material showing no electrochemically active surface (Fig. 1c) and hence little potential for fuel cell use.

The effect of a hydride layer on the surface of bio-Pd must be considered; such a ‘masking’ layer underlies the choice of bio-Pt for detailed electrochemical studies (Attard et al. 2012). This phenomenon introduces an uncertainty as to whether interactions are taking place at the surface of the Pd crystals in a true catalytic process or as a result of hydride formation or H₂ absorbed within the crystal structure of the Pd-NPs. Electrochemical analysis was used (with this caveat); although cyclic voltammograms (CVs) from samples loaded with 20 % (w/v) Pd(0) made under H₂ exhibited electrochemically active areas proper quantification would require integration under the desorption peaks and corrections for scan rate and nominal charge per cm² for the Pd. This is not trivial. However the response was observed regardless of the Pd salt used (Fig. 1a, b). Bio-Pd_{E. coli} also showed relatively small capacitance and resistance when compared to bio-Pd_{Shewanella oneidensis} (Fig. 3a). Comparing Figs. 1 and 3, it appears that the capacitance shown by the bio-Pd_{E. coli} is ~0.5–0.6 microamps whereas that of bio-Pd_{S. oneidensis} is ~twice this value. The resistance also appears slightly lower in bio-Pd_{E. coli} due to the less sloping baselines to the voltammetry. Note that these are (approximate) observations made directly from the voltammetry and no separate measurements have been made to quantify them.

In contrast to CVs obtained from H₂-derived bio-Pd (Figs. 1a, b, 3a), bio-Pd made using formate shows no significant electrochemical interaction using either cell type (Figs. 1c, 3b). The Pd-NPs made from

formate were held apart by biomass materials (Fig. 2b, c); hence this study shows no intrinsic conductivity via biomass layers between the Pd-NPs of intact cells. In contrast bio-Pd made under H₂ was electrically conductive, possibly attributed to direct contact between adjacent Pd-NPs. Wu et al. (2011) argue for a role of Pd-NPs in extracellular electron transfer with, at high Pd-loading, no requirement for cellular metabolism since Pd(0) splits H₂ catalytically to yield electrons.

From Fig. 1a, b several conclusions can be inferred. The CVs show several ‘fingerprint’ peaks that are characteristic of proton adsorption occurring at the catalyst surface. As noted above the system used may lead to ambiguity due to the behaviour of protons towards Pd crystals. The possibility of proton absorption into the structures means the method cannot be used to assess conclusively the Pd-NP surface features (kinks, terraces etc.) or the electrochemical surface area as a true monolayer of protons may not be formed. However the method allows for comparison of the behaviour of Pd-NPs when compared between separate samples and it is notable that a difference in CV peaks was observed between bio-Pd(0) samples produced using formate or H₂ and also Na₂PdCl₄ and PdCl₂ as the palladium source, as well as between two species of bacteria that produced bio-Pd(0) at the expense of H₂ from PdCl₂ (Figs. 1a, 3a).

It is proposed that the reason underlying the observed differences between materials made using H₂ or formate is the size and relative positioning of bio-NPs. With formate, deposition appears to be relatively uniform across the cross sectional area of the cell surface, producing relatively small, unaggregated NPs, whereas under H₂ the deposition occurred preferentially at the cell membranes forming larger NPs (Fig. 1a, b) as aggregates (Fig. 2a). During electrochemical analysis the latter produced larger signals, with a much larger associated non-faradaic charge transfer. Nominally this indicates a higher surface area available for electrocatalytic reaction, however due to the size of the NPs it may be associated with a larger volume of proton adsorption within them.

A repeated voltage scan (e.g. from samples using H₂ for bio-Pd manufacture from PdCl₂; Figs. 1a, 3a) shows CVs recorded during repeated scans, each experiment representing several additional voltage cycles. There are several possible explanations for an observed change in the desorption peak at E⁰

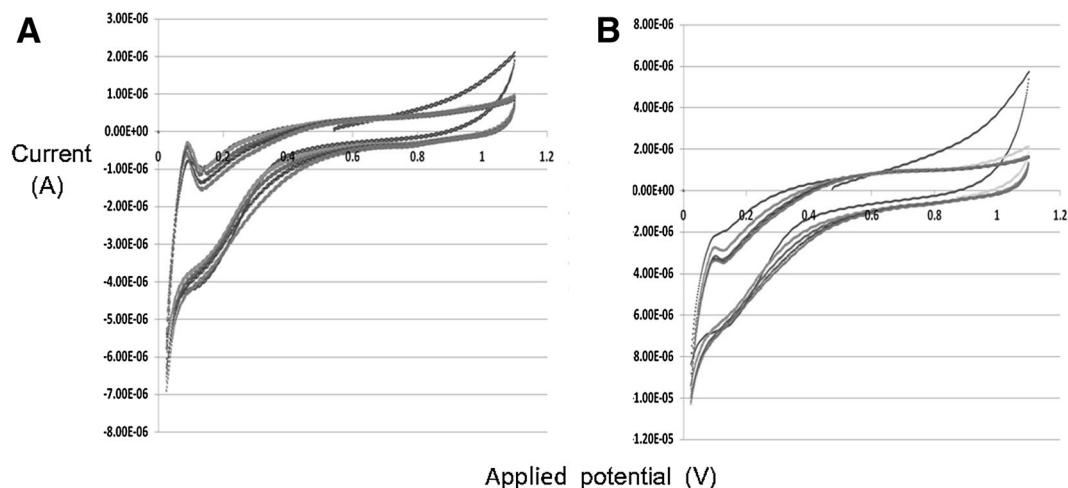


Fig. 3 Cyclic voltammograms of cell preparations of bio-Pd on *S. oneidensis* made from PdCl_2 at the expense of H_2 (a) and formate (b) as described for *E. coli*

0.05–0.2 V seen in Fig. 1a. It is possible that poisoning of the catalyst surface occurred via impurities in the electrolyte or compounds associated with the bacterial surface (note that such changes were also seen when experiments were repeated using different commercial sources of perchloric acid and alternative sources of distilled water). Other studies have confirmed using bio-Pt that even material ‘cleaned’ using NaOH contains a component of residual cellular material which, when removed via further chemical cleaning and then electrochemical removal of the final residua, leads to unmasking of various additional features in the CV from which information about the actual crystal surface can then be obtained (Attard et al. 2012). A similar analysis is not possible using bio-Pd due to the masking effect of the H_2 chemistry at the catalyst surface (above). However, it could be hypothesised through analysis of the CVs that a 110 crystal surface, which initially produces the largest charge transfer, becomes poisoned and that the 100 surface increases in dominance. This may be enhanced by the 100 surface being electrochemically ‘cleaned’; such progressive cleaning results in loss of electrochemical resolution due to nanoparticle aggregation (Attard et al. 2012).

Yong et al. (2007) noted little activity of bio-Pt or bio-Pd per se as an oxidation catalyst in a PEM-FC anode and that sintering was required to carbonise the material in order to confer conductivity. In contrast the present study suggests that the biomass residua may, in

fact, be electrically conductive given sufficient charge accumulation to overcome the ohmic resistance.

Acknowledgments JC was in receipt of an EPSRC studentship via the EPSRC Doctoral Training Centre ‘ H_2 , Fuel Cells and Their Applications’ This work was supported by EPSRC Grant No EP/H029567/1.

Open Access This article is distributed under the terms of the Creative Commons Attribution 4.0 International License (<http://creativecommons.org/licenses/by/4.0/>), which permits unrestricted use, distribution, and reproduction in any medium, provided you give appropriate credit to the original author(s) and the source, provide a link to the Creative Commons license, and indicate if changes were made.

References

- Attard GA, Casadesus M, Macaskie LE, Deplanche K (2012) Biosynthesis of platinum nanoparticles by *E. coli* MC4100: can such nanoparticles exhibit enantioselectivity? *Langmuir* 28:5267–5274
- De Windt W, Aelterman P, Verstraete W (2005) Bioreductive deposition of palladium (0) nanoparticles on *Shewanella oneidensis* with catalytic activity towards reductive dechlorination of polychlorinated biphenyls. *Environ Microbiol* 7:314–325
- De Windt W, Boon N, Van der Bulckes J et al (2006) Biological control of the size and reactivity of catalytic Pd(0) produced by *Shewanella oneidensis* Antonie Van Leeuwenhoek Int J Gen. Mol Microbiol 90:377–389
- Deplanche K, Caldari I, Mikheenko IP et al (2010) Involvement of hydrogenases in the formation of highly catalytic Pd(0) nanoparticles by bioreduction of Pd(II) using

Escherichia coli mutant strains. *Microbiology* 156: 2630–2640

Dimitriadis S, Nomikou N, McHale AP (2007) Pd-based electrocatalytic materials derived from biosorption processes and their exploitation in fuel cell technology. *Biotechnol Lett* 29:545–551

Jang JK, Kan J, Bretschger O, Gorby YA et al (2013) Electricity generation by a microbial fuel cell using microorganisms as catalyst in cathode. *J Microb Biotechnol* 23:1765–1773

Macaskie LE, Baxter-Plant VS, Creamer NJ et al (2005) Applications of bacterial hydrogenases in waste decontamination, manufacture of novel bionanocatalysts and in sustainable energy. *Biochem Soc Trans* 33:76–79

Mikheenko IP, Rousset M, Dementin S et al (2008) Bioaccumulation of palladium by *Desulfovibrio fructosivorans* wild-type and hydrogenase-deficient strains. *Appl Environ Microbiol* 74:6144–6146

Ogi T, Honda R, Tamaoki K et al (2010) Biopreparation of highly dispersed Pd nanoparticles on bacterial cells and their catalytic activity for polymer electrolyte fuel cell. *MRS Proc.* doi:[10.1557/PROC-1272-PP06-03](https://doi.org/10.1557/PROC-1272-PP06-03)

Ogi T, Honda R, Tamaoki K et al (2011) Direct room temperature synthesis of a highly dispersed palladium nanoparticle catalyst and its electrical properties in a fuel cell. *Powder Technol* 205:143–148

Orozco RL, Redwood MD, Yong P et al (2010) Towards an integrated system for bio-energy: hydrogen production by *Escherichia coli* and use of palladium-coated waste cells for electricity generation in a fuel cell. *Biotechnol Lett* 32:1837–1845

Redwood MD, Orozco RL, Majewski AJ, Macaskie LE (2012) An integrated biohydrogen refinery: synergy of photofermentation, extractive fermentation and hydrothermal hydrolysis of food wastes. *Biores Technol* 119:384–392

Rice CA, Urchaga P, Pistrone AO et al (2015) Platinum dissolution in fuel cell electrodes: enhanced degradation from surface area assessment in automotive accelerated stress test. *J Electrochem Soc* 162:F1175–F1180. doi:[10.1149/2.0371510jes](https://doi.org/10.1149/2.0371510jes)

Sanchez DVP, Jacobs D, Gregory K et al (2015) Changes in carbon electrode morphology affect microbial fuel cell performance with *Shewanella oneidensis* MR-1. *Energies* 8:1817–1829

Søbjerg LS, Lindhardt AT, Skrydstrup T et al (2011) Size control and catalytic activity of bio-supported palladium nanoparticles. *Coll Surf B* 85:373–378

Williams AR (2016) Biogenic precious metal based magnetic nanocatalyst for enhanced O₂ reduction. PhD Thesis University of Birmingham UK

Wu X, Zhao F, Rahunen N et al (2011) A role for microbial palladium nanoparticles in extracellular electron transfer. *Ang Chemie* 123:447–450

Wu W, Yang F, Liu X, Bai L (2014) Influence of substrate on electricity generation of *Shewanella loihica* PV-4 in microbial fuel cells. *Microb Cell Fact* 13:69–75

Wu G, Li N, Mao Y, Zhou G, Gao H (2015) Endogenous generation of H₂S and its regulation in *Shewanella oneidensis*. *Front Microbiol* 6: article 374. doi:[10.3389/fmicb.2015.00374](https://doi.org/10.3389/fmicb.2015.00374)

Yong P, Paterson-Beedle M, Mikheenko IP, Macaskie LE (2007) From bio-mineralisation to fuel cells: biomanufacture of Pt and Pd nanocrystals for fuel cell catalysts. *Biotechnol Lett* 29:539–544

Yong P, Mikheenko IP, Deplanche K et al (2010) Biorefining of precious metals from waste: an answer to manufacturing of cheap catalysts for fuel cells and power generation via an integrated biorefinery? *Biotechnol Lett* 32:1821–1828

Zhu J, Wood J, Deplanche K et al (2016) Selective hydrogenation using palladium bioinorganic catalyst. *Appl Catal B. Environ* (in press)